Negative helium ions exiting a carbon foil at keV energies

H. O. Funsten,* S. M. Ritzau, and R. W. Harper
Los Alamos National Laboratory, Los Alamos, New Mexico 87545

(Received 19 January 2000; revised manuscript received 30 October 2000; published 30 March 2001)

He^- is observed in the exit charge state distributions of He transmitted through a thin carbon foil over an energy range of 8–80 keV. The observed exit fraction of He^- must be formed in the bulk foil or within several Angstroms of the exit surface and reaches a maximum of 2.6×10^{-4} at $0.7v_0$ where v_0 is the Bohr velocity. The probability of forming the observed He^- from its source population of He^+ by two sequential electron-capture events decreases exponentially with increasing velocity. This behavior is similar to that of He transiting a Cs vapor, for which this dependence is the result of individual cross sections that collectively drive the charge-state distribution toward higher positive-charge states with increasing projectile velocity. No isotope effect in the exit charge state distributions of ^3He and ^4He is observed within experimental error.

DOI: 10.1103/PhysRevB.63.155416 PACS number(s): 79.20.Rf, 34.50.Fa, 34.50.Dy, 41.75.Ak

I. INTRODUCTION

Owing to the simple two-electron system of neutral He, the experimental study of the formation of He^- using interactions of energetic He beams with charge-exchange vapors has provided a superb method for gauging the accuracy of theoretical atomic models.[1–3] These results show that the fraction of a He beam exiting a vapor charge exchange cell as He^- is highest for alkali metal vapors.[4–7] The relatively high yield of He^- is due to the near-resonance of the shallow electron affinity energy level of He^- and the first ionization potential of the alkali metal atom, enabling relatively efficient charge-transfer to form He^-. This result forms the basis of alkali metal ion sources for production of He^- in accelerators.[4,8]

He^- has also been observed as a reflected charge state resulting from He^+ incident on a Na target,[9] which has a relatively low work function of 2.75 eV.[10] In these studies, the energy distribution of the reflected He^- was strongly dependent on the energy of the incident He^+. This was attributed to a close collision of He with a Na atom that resulted in a recoiling, excited neutral He that was a precursor to the formation of He^- along the outbound trajectory.

In contrast to the reflection studies, a beam of He exiting a foil has a narrow scatter distribution, so few, if any, ions undergo large-angle scattering events. Consequently, the exit charge-state distribution of He includes very few ions that have encountered a close collision with a target nucleus, and the observed exit charge state distribution is governed only by the equilibrium charge state distribution in the bulk foil and charge exchange processes at the exit surface. Coupled with the comparatively high work function of a carbon foil relative to a pure Na target and the shallow affinity level of He^-, we use this study to elucidate the formation kinetics of He^- observed in the exit charge state distribution of He transmitted through an ultrathin carbon foil.

II. EXPERIMENT

The experimental apparatus used to measure the exit charge state distribution is shown schematically in Fig. 1. A 1-mm-diameter, magnetically mass-analyzed beam of He^+ at incident energy E was directed at normal incidence onto a thin (nominal 0.5 $\mu g/cm^2$) carbon foil. The exiting beam transited a 0.35-mm-wide slit aperture located 5.8 mm from the foil and then passed through parallel electrostatic deflection plates that spatially separated the ions according to their exit charge state q. The ions were then detected using a position-sensitive microchannel plate (MCF) detector located 12.6 cm from the foil. The total number of counts $C(He^-)$ detected within the detector area associated with each spatially separated charge-state distribution was measured. The distance of 9.2 cm from the foil to the end of the deflection plates corresponded to 149 ns for 8-keV ^4He, which is 60 times less than the shortest lifetime of He^-, which is metastable. Therefore, few He^- decay before they are deflected toward the location at which He^- is detected at the MCP detector.

The measured exit fraction of He^0, defined as $f(He^0)$, was always several orders of magnitude greater than the exit fractions of He^- and He^{2+}. For example, $f(He^0)=0.87$ compared to $f(He^+)=0.13$, $f(He^-)=2.6\times10^{-4}$, and $f(He^{2+})=5\times10^{-4}$ at $0.62v_0$, where v_0 is the Bohr velocity. This resulted in excess noise counts in the negative-ion distribution due to the proximity of the negative ions to the neutrals at the detector. Therefore, a metallic strip was mounted in front of the detector to block He^0 and maximize the signal-to-noise ratio during measurement of He^- and He^{2+}. In this configuration, the ratios of the exit fractions $f(He^-)/f(He^+)$ and $f(He^{2+})/f(He^+)$ were derived according to $f(He^q)/f(He^+)=C(He^q)/C(He^+)$. The strip was then removed, and the ratio $f(He^0)/f(He^+)=C(He^0)/C(He^+)$ was obtained. The exit fractions $f(He^-)$, $f(He^0)$, $f(He^+)$, and $f(He^{2-})$ were subsequently derived using these ratios and using the identity $f(He^-)+f(He^0)+f(He^+)+f(He^{2+})=1$. As previously reported,[11] the exit fraction $f(He^+)$ was proportional to the square of the projectile speed.

For the foil thickness used in this study, the exit scatter distribution had an angular half-width of $\sim3.5°$ at 10 keV and decreased as $1/E$ with increasing energy E.[11] From the angular scatter distributions, we infer a carbon foil thickness of approximately 1.1 $\mu g/cm^2$. Both the extrapolation to lower energies of the foil thickness that is required for charge

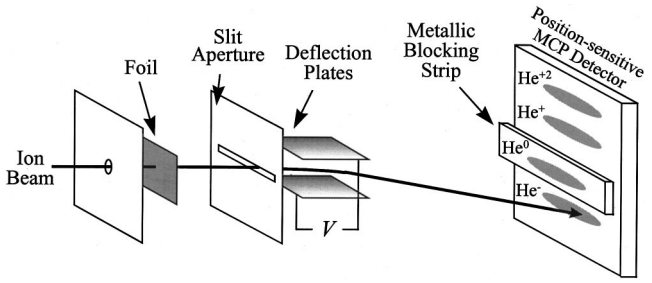

FIG. 1. The experimental apparatus used to measure the exit charge fractions of He consisted of a nominal 0.5 μg/cm^2 carbon foil followed by a slit aperture, electrostatic deflection plates, and a position-sensitive microchannel plate (MCP) detector. A metallic blocking strip was placed at the location of the dominant He^0 exit charge fraction in order to measure the exit fractions of He^- and He^{+2} relative to the exit fraction of He^+. The metallic strip was removed to measure the fraction of He^+ relative to He^0.

state equilibrium[12,13] and the measurements showing the independence of the exit charge state distribution on the incident charge state[14,15] indicate that charge-state equilibrium is achieved with a 1.1-μg/cm^2 foil at the energies used in this study.

III. RESULTS AND DISCUSSION

Figure 2 shows the measured exit fractions of $^3He^-$ and $^4He^-$, which increase with increasing velocity to a maximum value of 2.6×10^{-4} at $\sim0.7v_0$ and subsequently slowly decrease at higher velocities. This behavior is qualitatively similar to the fractions of H^- and C^- emerging from a carbon foil,[16] although the maxima of those negative ion fractions occur at much lower velocities ($0.36v_0$ for H^- and $0.28v_0$ for C^-). For the formation of H^- and C^-, the maxima in the exit fraction of negative ions are the result of two competing effects that act to limit the negative ion yield: resonant neutralization at the exit surface, which is dominant at low velocities, and a lower fraction of neutrals in the bulk foil, which are the seed population for negative ions, as the beam is driven to a higher positive charge at higher velocities.[16] In contrast, we show later that the seed population of He^- is He^+, so we expect that the maximum value of $f(He^-)$ would occur at a higher velocity at which a higher fraction of He^+ is present, as is observed.

Also shown in Fig. 2 is the exit fraction of $^4He^-$ for helium transmitted through a carbon foil over the energy range 60–250 keV measured by Kestelman, Alonso, and Baragiola.[17] These data generally agree with the data derived in this study at $0.76v_0$ but is $\sim$25% higher at $1.0v_0$. Within experimental error, Fig. 2 shows that the exit fractions of ^{3}He and ^{4}He are the same at equal velocities, indicating the absence of an isotope effect in the exit charge state distribution. This agrees with other studies that found no isotope difference in the exit charge state distributions of H and D (Ref. 18) and ^{20}Ne and ^{22}Ne (Ref. 14) transmitted through carbon foils.

To interpret our results, we ignore short-lived negative-ion resonances of He^- such as $1s2s\ ^2S(\sim10^{-14}\,\mathrm{s})$ (Ref. 19)

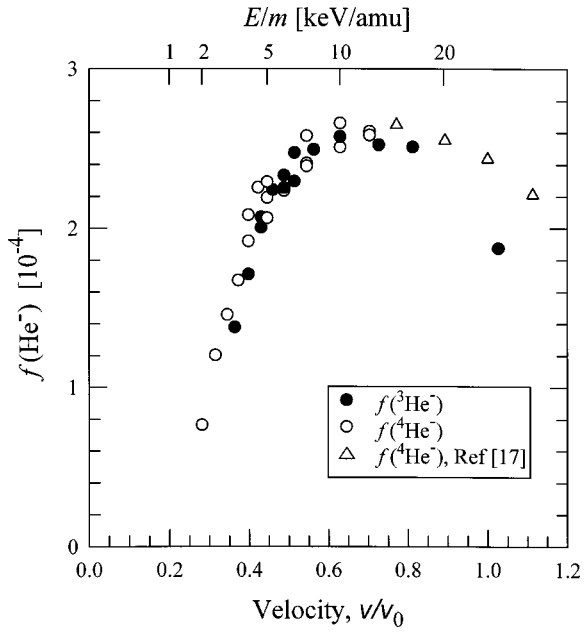

FIG. 2. The measured exit fraction of $^3He^-$ and $^4He^-$ is shown as a function of the projectile velocity relative to the Bohr velocity v_0. With increasing velocity, these exit fractions increase toward a maximum of 2.6×10^{-4} at $0.7v_0$ and subsequently decrease. The open triangles are data from Kestelman, Alonso, and Baragiola (Ref. 17).

and instead focus on the long-lived $1s2s2p\ ^4P^0$ state of He^- that can be created from the following two-step, spin-conserving charge exchange process

$$(1s\ ^2S)\mathrm{He}^+ \xrightarrow{\mathrm{EC}} (1s2s\ ^3S)\mathrm{He} \xrightarrow{\mathrm{EC}} (1s2s2p\ ^4P^0)\mathrm{He}^-, \quad (1)$$

where EC represents electron capture from a third body.[2,5] The resulting doubly excited, metastable He^-, which decays by spin-dependent interactions, is long lived ($\sim$8.9 μsec lifetime for the $^4P_{1/2}$ and $^4P_{3/2}$ states and $\sim$343 μsec for the $^4P_{5/2}$).[20] Using Eq. (1) as a basis for He^- formation, the source population of He^- observed in the exit charge state distribution is He^+ in the bulk foil.

Far from the foil surface, a $(1s2s2p\ ^4P^0)He^-$ atom has an affinity level $E_A=-0.0775$ eV,[3] and the excited $2s\ ^3S$ state of He^+ has an energy level $E_{2S}=-4.76$ eV (Ref. 21) relative to the vacuum level. Close to the foil surface, E_A and E_{2S} are significantly shifted due to the image-charge potential.[22] The level shift is approximately[23]

$$E(s)=E(\infty)\pm\frac{e^2}{s}, \quad (2)$$

where s is approximately the distance from the ion to the image plane and the sign depends on the ion charge: $E(s)$ shifts level upward [+ in Eq. (2)] for the case of a positive ion, and $E(s)$ shifts downward [− in Eq. (2)] for a negative ion. Figure 3 qualitatively illustrates the level shifts of the (filled) affinity level $E_A(s)$ of $(1s2s2p\ ^4P^0)He^-$ and the (empty) energy level $E_{2S}(s)$ of the excited $2s\ ^3S$ state of He^+ in the vicinity of a conductor. Equation (2) is generally accurate for s greater than several Angstroms from the image

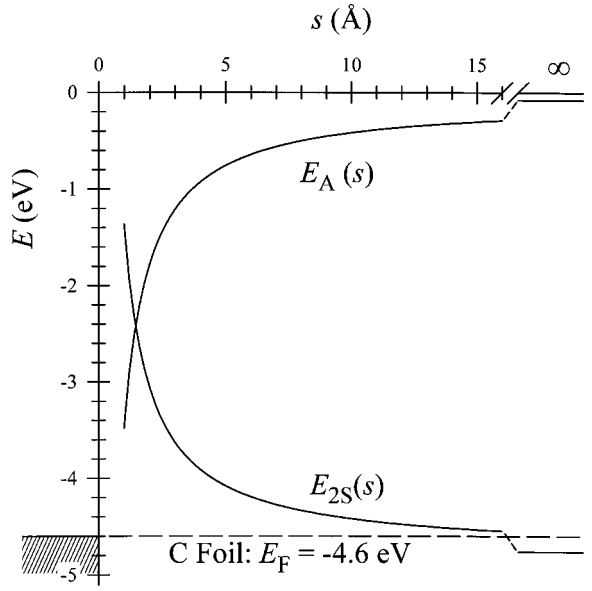

FIG. 3. The shifts of the affinity level E_A(s) of He^- and the $2s$ level E_{2S}(s) of He^+ due to the image potential are shown in the vicinity of a conductor. Except for E_{2S}(s) at large distances from the foil, these levels are never in resonance with the filled valence band of the carbon foil, which likely has a work function similar to that of graphitic carbon (−4.6 eV) (Ref. 25). This figure qualitatively illustrates that formation of He^- several angstroms beyond the image plane is prohibited due to the absence of resonance of the E_A and E_{2S} levels with filled valence states in the foil.

plane and corresponds to the region in which resonant charge exchange and Auger processes occur. In addition to this shift, the atomic levels widen (not shown in Fig. 3) due to Heisenberg broadening, enabling broader overlap between the atomic levels of the exiting He beam and filled or unfilled levels in the foil.[24]

We assume that the work function of the carbon foil is equal to that of graphitic carbon ($E_F \approx -4.6$ eV),[25] which is shown in Fig. 3. In the vicinity of the surface where charge exchange might occur (e.g., $s<10$), the E_{2S} level shifts out of resonance with the filled valence states of the foil and E_A shifts toward, but is never in resonance with, the filled valence states. While Heisenberg broadening may contribute to degeneracy of E_A and formation of He^- very close to the surface, broadening of the E_{2S} level decreases exponentially with increasing distance s. Overlap of the E_{2S} level with the filled valence states in the foil will occur only at a large distance s at which E_A is far from the Fermi level. Therefore, the formation of the He^- via Eq. (1) must occur in the bulk foil or in the immediate vicinity (within a few angstroms) of the image plane.

Using the sequential electron capture processes described by Eq. (1), the probability of forming He^- is the product of the equilibrium fraction $f_B(He^+)$ of He projectiles in the bulk foil that are singly ionized, the probability P_{+-} of forming He^- from the seed population of He^+ near the image plane, and the survival probability P_S of He^- as it moves away from the image plane. Therefore, the observed fraction of He exiting the foil as He^- is

$$f(He^-) = f_B(He^+) P_{+-} P_S . \tag{3}$$

We now examine these parameters and their contributions to the observations of $f(He^-)$.

The observed exit fraction $f(He^+)$ can be different from the bulk fraction $f_B(He^+)$ if He^+ emerging from the bulk is efficiently neutralized at the exit surface. This might occur through resonant neutralization to the $2s$ level of He^+, which may be followed by Auger deexcitation; resonant neutralization between core levels of the carbon foil and the $1s$ state of He; or direct Auger neutralization into the ground state of He accompanied by excitation of a second valence electron in the foil. The first two processes are unlikely: resonant transfer to the $2s$ level of He^+ near the surface is prevented by the shift of E_{2S} far from resonance with the valence levels in the foil, and resonant transfer to the $1s$ state of He^+ requires a close collision,[26] which is an infrequent event as indicated by the small angular scattering of He emerging from the foil. The third process, direct Auger neutralization (AN), might occur. In this case, the observed exit fraction of He^+ that survives direct AN is $f(He^+) = f_B(He^+)\exp(-v_{AN}/v)$, where v_{AN} is the AN transition rate integrated over the trajectory of the ion beyond the surface and v is the ion velocity perpendicular to the surface.[27]

Resonant neutralization (RN) of He^- can occur via resonant tunneling of the electron in the affinity level to unfilled states in the conduction band. The survival probability of He^- against this process is $P_S = \exp(-v_{RN}/v)$, where v_{RN} is the integrated RN transition rate over the ion's trajectory beyond the surface.[24]

Including both direct AN of He^+ and RN of He^-, the ratio of the observed exit fraction of He^- to the observed exit fraction of He^+ is

$$\frac{f(He^-)}{f(He^+)} = \exp\left(\frac{v_{AN} - v_{RN}}{v}\right) P_{+-} . \tag{4}$$

The ratio $f(He^-)/f(He^+)$ is shown in Fig. 4 for both ^{3}He and ^{4}He and exhibits a clear exponential dependence on the projectile velocity. A least-square fit to the data of this study yields

$$\frac{f(He^-)}{f(He^+)} = 0.0194 \exp\left(-3.61 \frac{v}{v_0}\right), \tag{5}$$

which is shown as the solid line in Fig. 4. The open triangles in the figure were derived using the measured exit fractions of He^- from Kestelman, Alonso, and Baragiola[17] and extrapolated values of the exit fractions of He^+ from Funsten, McComas, and Barraclough.[11] These values of the ratio $f(He^-)/f(He^+)$ slightly deviate from the exponential dependence at the highest velocities. Errors in these values might be expected since they were derived using different foils and different experimental apparatus and techniques.

If either RN of He^- or AN of He^+ was a dominant process, then the ratio $f(He^-)/f(He^+)$ would appear nonlinear in the semilogarithmic plot of Fig. 4, which is not observed. Furthermore, if RN of He^- was dominant, then the ratio

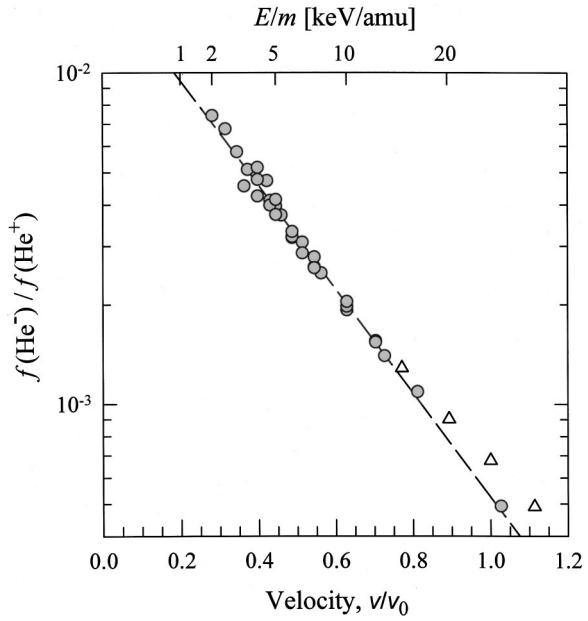

FIG. 4. The ratio of the observed exit fractions of He^- and He^+ (filled gray circles) is shown as a function of the incident projectile velocity for He exiting a carbon foil. The ratio, which is proportional to P_{+-} based on Eq. (3) and the subsequent analysis, decreases exponentially with increasing velocity. The solid line is a fit to the data and corresponds to $f(He^-)/f(He^+)=0.0194\exp(-3.61v/v_0)$. The open triangles are based on a combination of He^- data from Kestelman, Alonso, and Baragiola (Ref. 17) and He^+ data from Funsten, McComas, and Barraclough (Ref. 11).

would increase with increasing velocity as more He^- survive RN, which is the opposite of the trend observed in Fig. 4. Consequently, both AN of He^+ and RN of He^- are either insignificant over the velocity range of this study or are significant but cancel each other (i.e., $v_{AN}\approx v_{RN}$) so that their individual effects cannot be observed. We expect the former to be true since AN is generally a process that is observed at slow velocities; for example, calculations indicate that $v_{AN}\approx 0.03v_0$ for He^+ exiting Al^{28} which is considerably less than the lowest projectile speed in this study. We therefore conclude that the measured fraction $f(He^+)$ mirrors that of the bulk foil [i.e., $f(He^+)\approx f_B(He^+)$] and that $P_{+-}\propto\exp(-3.61v/v_0)$.

Some insight into P_{+-} might be obtained by developing charge-exchange equations to represent Eq. (1). For simplicity and for comparison with results of He incident on a Cs vapor target, we assume equilibrium charge state distributions for these charge-exchange equations. While the observed He^- may result from modification of equilibrated bulk charge state distributions near the exit surface of the foil, the results of this analysis are, interestingly, similar to the equilibrium fraction of He^- transiting a Cs vapor.

The He system consists of five charge-state components [doubly positive (+2), singly positive (+), neutral singlet (*s*), neutral triplet $1s2s\ ^3S(t)$, and negative(−)], although we can greatly simplify the system by considering the large differences in the magnitudes of the charge state fractions and by imposing some restrictions on charge-exchange processes.

(1) $f(He^{+2})\ll f(He^+)$: Since the He^{+2} component is so small and does not contribute to formation of He^-, we ignore $f(He^{+2})$.

(2) $f(He^0)\gg f(He^+)$: Since He^+ is the seed population for the triplet state $1s2s\ ^3S$ He, then $f(He^+)$ is likely larger than the fraction of He^0 in the triplet state. Therefore, $f(He^0)$ is populated primarily by neutrals in the ground state rather than in the triplet state, and $f(He^+)$ is governed primarily by charge exchange with these ground-state neutrals. This two-component system results in $f(He^+)=f(He^0)\sigma_{S+}/\sigma_{+S}$, where σ_{ij} is the charge exchange cross section from charge state *i* to charge state *j*, and the subscript *s* refers to singlet He^0.

(3) We assume double-electron capture or loss cannot occur within a single interaction. Also, according to Eq. (1) ground-state He^0 cannot form triplet He^0 or He^- in a single charge exchange event.

The result, which also follows directly from Eq. (1), is a three-component system that leads to formation of He^- from a source population of He^+ that itself is governed by the fraction of singlet He^0. The probability of forming He^- from He^+ is therefore

$$\frac{f(He^-)}{f(He^+)}=\frac{\sigma_{+t}\sigma_{t-}}{(\sigma_{t+}+\sigma_{t-}+\sigma_{ts})\sigma_{-0}}=P_{+-}, \qquad (6)$$

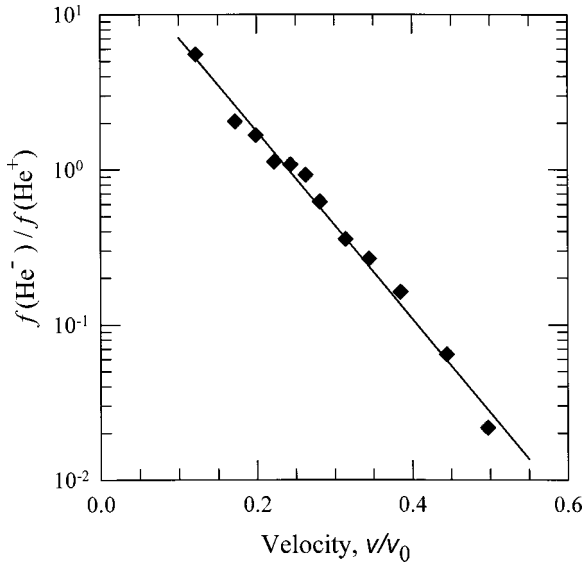

FIG. 5. The ratio of the equilibrium charge fractions $f(He^-)$ and $f(He^+)$ for He transiting a Cs vapor target decreases exponentially with increasing velocity, similar to the case of He transiting a solid carbon foil shown in Fig. 4. The equilibrium charge fractions were calculated using measured charge exchange cross sections (Ref. 6). The solid line is a fit to the data and corresponds to $f(He^-)/f(He^-)=28.4\exp(-13.9v/v_0)$.

where the subscript 0 includes both the singlet (s) and triplet (t) states of He^0. This equation relates P_{+-} directly to equilibrium charge exchange cross sections. We note that the numerator consists of cross sections leading to the formation of He^-, and the denominator contains cross sections that represent destruction of states that result in the formation of He^-.

Comparison of the interactions of He in solid and gaseous targets can be quite perilous due to the pronounced differences in the interaction kinetics of the two types of targets, including a shorter path length between sequential interactions in a solid (the density effect)[12] and substantial screening of the projectile within a solid.[29,30] Nevertheless, we note that the fraction of He^- emerging from alkali vapor targets has been studied extensively,[6,7] and Schlachter *et al.*[6] derived charge-exchange cross sections for He transiting a Cs vapor target. Using the change in the three-component $(+, 0, -)$ charge-state distribution for different target thicknesses, they inferred cross sections for the four-component system having neutral singlet and neutral triplet states.

Figure 5 shows the ratio $f(He^-)/f(He^+) = \sigma_{+0}\sigma_{0-}/\sigma_{0+}\sigma_{-0}$ as a function of He velocity based on the cross sections derived using the three-component system and assuming an equilibrium charge state distribution. The data clearly exhibit an exponential decrease of the ratio $f(He^-)/f(He^+)$ with increasing velocity, which is the same dependence as that found in this study using a carbon foil target and shown in Fig. 4. The solid line in Fig. 5 is a fit to the data and corresponds to $f(He^-)/f(He^+) = 28.4 \exp(-13.9v/v_0)$. The decrease in $f(He^-)/f(He^+)$ with increasing velocity is driven primarily by the increase in the cross section σ_{0+} for formation of He^+ from He^0, which increased by a factor of ~ 20 from $0.12v_0$ to $0.49v_0$, while both σ_{+0} and σ_{0-} decreased by a factor of ~ 4 over the same velocity range (σ_{-0} remained approximately constant). Each of these cross sections reflect the tendency to drive the charge-state distribution more positive, collectively resulting in an exponential decrease in the ratio $f(He^-)/f(He^+)$. This is also likely the case for He transmission through a carbon foil.

In summary, we have measured the exit fraction of He^- emerging from a thin carbon foil. The fraction emerging from the foil as negative ions reaches a maximum value of 2.6×10^{-4} at $\sim 0.7v_0$, which is at least twice the velocity of the maximum negative-ion fraction observed for H^- and C^- projectiles emerging from a similar carbon foil. Based on the apparent absence of a net influence on the exit charge state distribution by Auger and resonant charge exchange processes at the exit surface, the probability of forming He^- from the seed population of He^+ is found to decrease exponentially with increasing velocity. This exponential dependence is also observed in He transiting a Cs vapor target, which is governed by cross sections that collectively drive the mean charge state distribution more positive with increasing velocity.

ACKNOWLEDGMENTS

This work was performed under the auspices of the United States Department of Energy. The authors gratefully acknowledge the laboratory assistance provided by J. Baldonado and D. Everett.

*Corresponding author. Mailing address: MS D466, Los Alamos National Laboratory, Los Alamos, New Mexico 87545. FAX: (505)665-7395. Email address: hfunsten@lanl.gov

[1] J. L. Pietenpol, Phys. Rev. Lett. **7**, 64 (1961); L. M. Blau, R. Novick, and D. Weinflash, *ibid.* **24**, 1268 (1970); G. N. Estberg and R. W. LaBahn, *ibid.* **24**, 1265 (1970); C. A. Nicolaides, Y. Komninos, and D. R. Beck, Phys. Rev. A **24**, 1103 (1981); A. V. Bunge and C. F. Bunge, *ibid.* **30**, 2179 (1984); T. Anderson, L. H. Anderson, P. Balling, H. K. Haugen, P. Hveplund, W. W. Smith, and K. Taulbjerg, *ibid.* **47**, 890 (1993).

[2] G. D. Alton, R. N. Compton, and D. J. Pegg, Phys. Rev. A **28**, 1405 (1983).

[3] P. Kristensen, U. V. Pedersen, V. V. Petrunin, and T. Andersen, Phys. Rev. A **55**, 978 (1997).

[4] R. M. Ennis, D. E. Schechter, G. Thoeming, D. B. Schlafke, and B. Donnally, IEEE Trans. Nucl. Sci. **14**, 75 (1967).

[5] B. L. Donnally and G. Thoeming, Phys. Rev. **159**, 87 (1967).

[6] A. S. Schlachter, D. H. Loyd, P. J. Bjorkholm, L. W. Anderson, and W. Haeberli, Phys. Rev. **174**, 201 (1968).

[7] H. B. Gilbody, R. Browning, K. F. Dunn, and A. I. McIntosh, J. Phys. B **2**, 465 (1969); T. Nagata, J. Phys. Soc. Jpn. **39**, 1334 (1975); R. J. Girnius and L. W. Anderson, Nucl. Instrum. Methods Phys. Res. **137**, 373 (1976).

[8] F. A. Rose, P. B. Tollefsrud, and H. T. Richards, IEEE Trans. Nucl. Sci. **14**, 78 (1967); T. John, C. P. Robinson, J. P. Aldridge, W. J. Wallace, K. R. Chapman, and R. H. Davis, *ibid.* **14**, 82 (1967); M. Sasao, A. Taniike, M. Nishiura, and M. Wada, Rev. Sci. Instrum. **69**, 1063 (1998).

[9] P. J. Schneider, W. Eckstein, and H. Verbeek, Nucl. Instrum. Methods Phys. Res. B **2**, 525 (1984); H. Verbeek, W. Eckstein, and P. J. Schneider, in *Production and Neutralization of Negative Ions and Beams*, edited by K. Prelec, AIP Conf. Proc. No. 111 (AIP, New York, 1984) pp. 273–280.

[10] R. J. Whitefield and J. J. Brady, Phys. Rev. Lett. **26**, 380 (1971).

[11] H. O. Funsten, D. J. McComas, and B. L. Barraclough, Opt. Eng. **32**, 3090 (1993).

[12] H. D. Betz, in *Applied Atomic Collision Physics*, edited by S. Datz (Academic, New York, 1983), pp. 1–42.

[13] V. P. Zaikov, E. A. Kral'kina, N. F. Vorobjev, I. S. Dmitriev, V. S. Nikolaev, and Ya. A. Teplova, Nucl. Instrum. Methods Phys. Res. B **5**, 10 (1984).

[14] A. Bürgi, M. Oetliker, P. Bochsler, J. Geiss, and M. A. Coplan, J. Appl. Phys. **68**, 2547 (1990).

[15] A. Bürgi, M. Gonin, M. Oetliker, P. Bochsler, J. Geiss, T. Lamy, A. Brenac, H. J. Andrä, P. Roncin, H. Laurent, and M. A. Coplan, J. Appl. Phys. **73**, 4130 (1995).

[16] H. O. Funsten, Phys. Rev. B **52**, R8703 (1995).

[17] A. J. Kestelman, E. Alonso, and R. A. Baragiola, IEEE Trans. Nucl. Sci. **NS-23**, 1143 (1976).

[18] S. Kreussler and R. Sizmann, Phys. Rev. B **26**, 520 (1982).

[19] G. L. Shultz, Rev. Mod. Phys. **45**, 378 (1973); S. J. Buckman and C. W. Clark, *ibid.* **66**, 539 (1994).

[20] A. Wolf, K. G. Bhushan, I. Ben-Itzhak, N. Alstein, D. Zajfman, O. Heber, and M. L. Rappaport, Phys. Rev. A **59**, 267 (1999).
[21] J. Roussel, Phys. Scr., T **T4**, 96 (1983).
[22] H. Jouin, F. A. Gutierrez, and C. Harel, Surf. Sci. **417**, 18 (1998).
[23] J. A. Appelbaum and D. R. Hamann, Phys. Rev. B **6**, 1122 (1972); N. D. Lang and W. Kohn, *ibid.* **7**, 3541 (1973).
[24] R. Brako and D. M. Newns, Rep. Prog. Phys. **52**, 655 (1989); J. Los and J. J. C. Geerlings, Phys. Rep. **190**, 133 (1990).
[25] F. R. McFeely, S. P. Kowalczyk, L. Ley, R. G. Cavell, R. A. Pollak, and D. A. Shirley, Phys. Rev. B **9**, 5268 (1974).
[26] R. Souda and M. Aono, Nucl. Instrum. Methods Phys. Res. B **15**, 114 (1986); R. Souda and K. Yamamoto, *ibid.* **125**, 256 (1997).
[27] E. C. Goldberg, R. Monreal, F. Flores, H. H. Brongersma, and P. Bauer, Surf. Sci. **440**, L875 (1999).
[28] W. More, J. Merino, R. Monreal, P. Pou, and F. Flores, Phys. Rev. B **58**, 7385 (1998).
[29] A. Arnau, Nucl. Instrum. Methods Phys. Res. B **93**, 195 (1994).
[30] P. M. Echenique, F. Flores, and R. H. Ritchie, in *Solid State Physics*, edited by H. Ehrenreich and D. Turnbull (Academic, New York, 1990), Vol. 43, pp. 229–308.